3D discrete dispersion relation, numerical stability and accuracy of the hybrid FDTD model for cold magnetized toroidal plasma

Maryna Surkova[1], Wouter Tierens[2], Ivan Pavlenko[3], Dirk Van Eester[4], Guido Van Oost[1], and Daniël De Zutter[2],
Fellow Member, IEEE

Abstract—The Finite-Difference Time-Domain (FDTD) method in cylindrical coordinates is used to describe electromagnetic wave propagation in a cold magnetized plasma. This enables us to study curvature effects in toroidal plasma. We derive the discrete dispersion relation of this FDTD scheme and compare it with the exact solution. The accuracy analysis of the proposed method is presented. We also provide a stability proof for nonmagnetized uniform plasma, in which case the stability condition is the vacuum Courant condition. For magnetized cold plasma we investigate the stability condition numerically using the von Neumann method. We present some numerical examples which reproduce the dispersion relation, wave field structure and steady state condition for typical plasma modes.

Index Terms—FDTD method, magnetized plasma, discretized dispersion relation, numerical stability, boundary conditions.

I. INTRODUCTION

THE finite-difference time-domain method is widely used to obtain solutions of Maxwell's equations for a broad range of electromagnetic problems [1, 2]. Especially, in the last two decades, the problems posed by modeling plasma waves have attracted a great deal of attention. A lot of research efforts have been spent over many years in order to improve the FDTD-methods to model wave propagation in different types of media and in particular in magnetized plasma such as the recursive convolution (RC) method [3 - 7] , the direct-integration (DI) method [8], the Z- transform method [9], the transmission line matrix method [10] and the split-step FDTD method [11]. An overview of the FDTD methods to model an isotropic cold plasma can be found in [12 - 13]. For more recent efforts on modeling the magnetized plasma the reader is referred to the work of Smithe [14], and enhancements along the lines of Smithe in [15], and [16]. Such methods generally fall in one of three categories: fully explicit ones [17], fully implicit ones [16], and hybrid ones [14], [15]. Fully explicit methods are straightforward and easy to implement but may suffer from restrictive stability conditions. Fully implicit methods are provably unconditionally stable but

[1] Department of Applied Physics, Ghent University, Sint-Pietersnieuwstraat 41 B4, 9000 Gent, Belgium. E-mail: maryna.surkova@UGent.be
[2] Electromagnetics Group, Department of Information Technology, Ghent University, Sint-Pietersnieuwstraat 41, 9000 Gent, Belgium
[3] Kharkiv Karazin National University, Department of Physics and Technology, Svobody sq., 4, Kharkiv, 61077, Ukraine
[4] Laboratory for Plasma Physics- ERM/KMS, "Association EURATOM-Belgia State", Renaissancelaan 30 Avenue de la Renaissance B-1000 Brussels, Belgium

require computationally intensive matrix calculations. In this light, hybrid methods seem an attractive option : they are stable at the relatively nonrestrictive vacuum Courant limit (though to our knowledge no general-case proof of this is known), and require only the solution of very small sets of equations every time step. These are the methods that we will use in this paper.

Both in flux tubes of the solar corona as in fusion devices, the geometry is basically toroidal. In this paper, wave propagation is studied adopting a toroidally symmetrical configuration.

In order to compare computational results with theoretical predictions (focusing on wave dynamics rather than wave interference), it is often convenient to suppress refections of the waves at the edge of the simulation region. For this purpose, an accurate and computationally efficient damping condition is needed [18- 20]. We will construct a simple but effective absorbing layer in this paper.

Of special interest is the case of fusion plasma when the antennas can launch different electromagnetic modes into the nonuniform plasma where they can tunnel through the evanescent layers or convert to the other modes. The plasma density increases from a very low magnitude near the antenna and the chamber conductive wall to very high on the magnetic axis. Usually the problems of the wave propagation through such structures are solved in the frequency domain. This approach eliminates the possibility to accurately describe the mode interactions and conversion. This is one of the reasons why the FDTD method has its merits for the study of problems in fusion plasma.

Generally speaking, the FDTD hot plasma description requires the solution of the kinetic equations instead of the current equations for plasma species. Constructing the current equations from the plasma conductivity tensor is also always problematic since the conductivity tensor is known only in the frequency domain [21]- [22].

Therefore we use the cold plasma approximation, which provides a fully local time-domain description for the plasma currents. Curvature effects are included by using the appropariate expression for the curl operator in cylindrical coordinates. After having grasped the cold plasma wave dynamics and having tested the suitability of the FDTD method, kinetic corrections can be incorporated to upgrade the adopted model. A similar approach to what will be presented in this paper is followed in [15]. Unlike [15] we will take curvature effects into account, and we use the Yee cell of [14], which differs from the one of [15].

After a short introduction and problem formulation in Section II, the description of the discretization scheme is provided in Section II-A. The associated discretized dispersion relation is derived explicitly in Section III, and special-case stability proofs are given. Section IV provides the accuracy analysis of the applied FDTD technique. Its stability for magentized plasma is discussed in Section V. A short description of the two implemented boundary conditions is presented in Section VI. Finally, in Section VII, some numerical examples are presented.

II. BASIC EQUATIONS AND DISCRETIZATION SCHEME

The cold plasma governing equations are cast in terms of Maxwell's equations coupled with current equations derived from the Lorentz equation of motion. The resulting whole governing equation set in time-domain is given by:

$$\frac{\partial \mathbf{B}}{\partial t} = -\nabla \times \mathbf{E}, \tag{1}$$

$$\epsilon_0 \frac{\partial \mathbf{E}}{\partial t} = -\sum_s \mathbf{J}_s + \nabla \times \mathbf{H}, \tag{2}$$

$$(\frac{\partial}{\partial t} + \nu_s)\mathbf{J}_s = \epsilon_0 \omega_{ps}^2 \mathbf{E} - \mathbf{\Omega}_s \times \mathbf{J}_s. \tag{3}$$

Here, the subscript s denotes the charged particle species in the plasma (e, i for electrons and ions respectively). $\mathbf{E}$ is the electric field vector (V/m), $\mathbf{B} = \mu_0 \mathbf{H}$ is the magnetic flux density vector (Wb/m^2), $\mathbf{H}$ is the magnetic field vector (A/m), $\mathbf{J}_s$ is the current density vector of a particular specie (A/m^2). The vacuum permeability μ_0 (H/m) and vacuum permittivity ϵ_0 (F/m) are independent of the frequency. The plasma frequency ω_{ps} (rad/sec) is defined as

$$\omega_{ps} = \sqrt{\frac{n_s q_s^2}{m_s \epsilon_0}} \tag{4}$$

where n_s ($1/m^3$), is the density, q_s (C), is the charge and m_s (kg), is the mass of a given specie. Further, by construction the cyclotron frequency is

$$\mathbf{\Omega}_s = \frac{q_s B_0}{m_s}, \tag{5}$$

where B_0 is the background magnetic field. Eq. (3) contains a collision frequency term whose role in the numerical simulations of experimental scenarios is fundamental. This term describes the power dissipation of the plasma currents due to the collision processes between the plasma particles. If it is small enough the wave damping is negligible, the wave power slightly decreases along the direction of the propagation and the wave field structure almost does not change.

A. Discretization Scheme

1) Time Discretization: We now introduce a finite- difference discretization of (1 - 3) and, following Yee's notation [1], we denote a mesh point as $(i, j, k) = (i\Delta, j\Delta, k\Delta)$, where $\Delta = \Delta r, \Delta\varphi, \Delta z$ is the space increment in the cylindrical coordinate system, and any function of space and time as $F^n(i, j, k) = F(i\Delta, j\Delta, k\Delta, n\Delta t)$, where Δt is the time

increment. By positioning the field components of $\mathbf{E}, \mathbf{H}, \mathbf{J}$ on the mesh the way that will be described below we evaluate the $\mathbf{E}$-field and the current density $\mathbf{J}$-field at integer time steps while the $\mathbf{H}$-field is defined at half-integer time steps [14]. By central averaging the $\mathbf{J}$ terms of Eq. (2) and Eq. (3) and the $\mathbf{E}$ term of Eq. (3), the resulting approximations of Eq. (1 - 3) are

$$\mu_0 \left[\frac{\mathbf{H}^{n+1/2} - \mathbf{H}^{n-1/2}}{\Delta t}\right] = -\nabla \times \mathbf{E}^n, \tag{6}$$

$$\epsilon_0 \left[\frac{\mathbf{E}^{n+1} - \mathbf{E}^n}{\Delta t}\right] + \left[\frac{\mathbf{J}_s^{n+1} + \mathbf{J}_s^n}{2}\right] = \nabla \times \mathbf{H}^{n+1/2}, \tag{7}$$

$$\left[\frac{\mathbf{J}_s^{n+1} - \mathbf{J}_s^n}{\Delta t}\right] + \nu_s \left[\frac{\mathbf{J}_s^{n+1} + \mathbf{J}_s^n}{2}\right] = \epsilon_0 \omega_{ps}^2 \left[\frac{\mathbf{E}^{n+1} + \mathbf{E}^n}{2}\right] - \left[\mathbf{\Omega}_s \times \frac{\mathbf{J}_s^{n+1} + \mathbf{J}_s^n}{2}\right]. \tag{8}$$

2) Space Discretization: The modified Yee-cell describing the spatial positioning of the $\mathbf{E}$-, $\mathbf{H}$-, and $\mathbf{J}_s$-field-components is shown in Fig. 1.
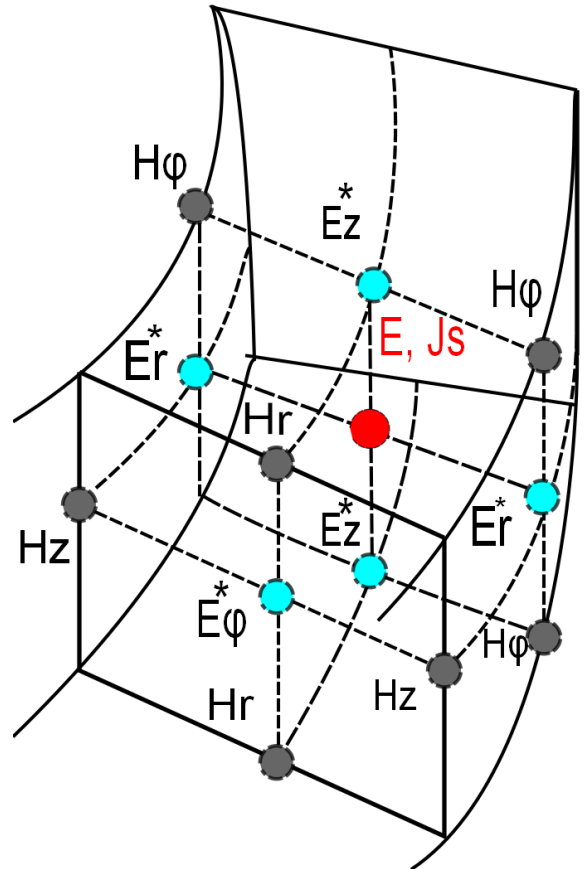
Fig. 1.   Yee cell for spatial positioning of the field components.

The components H_r, H_φ, H_z of the magnetic field $\mathbf{H}$ are localized at the center of the edges of the Yee- cell, as is typical in FDTD. The method proposed here initially locates the J_r, J_φ, and J_z components at the same positions as the E_r, E_φ, and E_z components, i.e. **together at the center of the Yee-cell** as in [14]. This simplifies the calculation of the cross product

in Eq.(3) while adding extra complexity to the calculation of the curl in Eq.(1): spatial averaging is required to calculate the central-difference derivatives. For example, to update the **H**-field components, four neighbouring field values of **E** should be averaged in order to find the field value at the centers of the faces of the Yee-cell. Thus, in order to interpolate the curl ($\nabla \times \mathbf{E}$), the twelve field values (four neighbouring values for each of the component) surrounding the desired position are then used to evaluate the corresponding derivative at that point. Unlike Eq. (6) (which is initially explicit), the set (7-8) is implicit. In order to obtain explicit expressions, the term $\mathbf{J}^{n+1}$ is defined from (8) and substituted in (7), which yields all of the field components of **E** at time step $(n + 1)$ on the left side of (9) and all other values calculated at previous time steps on the right- hand side of (9). As such, equation (9) becomes suitable for the FDTD implementation.

$$\mathbf{E}^{n+1} = \mathbf{M}_{E,E}\mathbf{E}^n - \mathbf{M}_{B,E} \sum_s \frac{1}{2}\left(\mathbf{M}_{2,s} + 1\right)\mathbf{J}^n$$
$$+ \mathbf{M}_{B,E}\left(\nabla \times \mathbf{H}\right)^{n+1/2}. \tag{9}$$

Using (9), the set of equations is completed with:

$$\mathbf{J}^{n+1} = \frac{\epsilon_0\omega_{ps}^2}{2}\mathbf{M}_{1,s}(\mathbf{M}_{E,E} + 1)E^n$$
$$- \frac{\epsilon_0\omega_{ps}^2}{2}\mathbf{M}_{1,s}\mathbf{M}_{B,E}\sum_s \frac{1}{2}\left(\mathbf{M}_{2,s} + 1\right)J^n \tag{10}$$
$$+ \frac{\epsilon_0\omega_{ps}^2}{2}\mathbf{M}_{1,s}\mathbf{M}_{B,E}\left(\nabla \times \mathbf{H}\right)^{n+1/2} + \mathbf{M}_{2,s}J^n,$$

where

$$\mathbf{M}_{1,s} = \begin{pmatrix} \frac{1}{\Delta t} + \frac{\nu_s}{2} & -\frac{\Omega_z}{2} & \frac{\Omega_\varphi}{2} \\ \frac{\Omega_z}{2} & \frac{1}{\Delta t} + \frac{\nu_s}{2} & -\frac{\Omega_r}{2} \\ -\frac{\Omega_\varphi}{2} & \frac{\Omega_r}{2} & \frac{1}{\Delta t} + \frac{\nu_s}{2} \end{pmatrix}^{-1}, \tag{11}$$

$$\mathbf{M}_{2,s} = \mathbf{M}_{1,s}\begin{pmatrix} \frac{1}{\Delta t} - \frac{\nu_s}{2} & \frac{\Omega_z}{2} & -\frac{\Omega_\varphi}{2} \\ -\frac{\Omega_z}{2} & \frac{1}{\Delta t} - \frac{\nu_s}{2} & \frac{\Omega_r}{2} \\ \frac{\Omega_\varphi}{2} & -\frac{\Omega_r}{2} & \frac{1}{\Delta t} - \frac{\nu_s}{2} \end{pmatrix}, \tag{12}$$

$$\mathbf{M}_{E,E} = \left(\frac{\epsilon_0}{\Delta t}I + \sum_s \mathbf{M}_{1,s}\frac{\epsilon_0\omega_{ps}^2}{2}\right)^{-1}\left(\frac{\epsilon_0}{\Delta t}I + \sum_s \mathbf{M}_{1,s}\frac{\epsilon_0\omega_{ps}^2}{2}\right), \tag{13}$$

$$\mathbf{M}_{B,E} = \left(\frac{\epsilon_0}{\Delta t}I + \sum_s \mathbf{M}_{1,s}\frac{\epsilon_0\omega_{ps}^2}{2}\right)^{-1}. \tag{14}$$

where I is a unit matrix.

III. DERIVATION OF THE FULL DISCRETE DISPERSION RELATION

The fully discretized dispersion relation derived in this Section relates the numerical wavevector components, the wave frequency, the time- and space-steps. Here, the basic procedure used for the dispersion analysis involves substitution of the expansion of the wave fields and plasma currents as a Fourier series in space and time into the discretized set of Maxwell's equations (6)-(8) using the cylindrical coordinate system. Initiating this procedure, we assume the following

solution, for example, for the electric field components in a form:

$$\mathbf{E}\big|_{\mathbf{r},\boldsymbol{\varphi},\mathbf{z}}^n =$$
$$= \frac{1}{2}\left[e^{(j(k_r\frac{\Delta r}{2}\mathbf{r}+n\frac{\Delta\varphi}{2}\boldsymbol{\varphi}+k_z\frac{\Delta z}{2}\mathbf{z}-\omega\frac{\Delta t}{2}\tau))}\right.$$
$$\left. + e^{(-j(k_r\frac{\Delta r}{2}\mathbf{r}+n\frac{\Delta\varphi}{2}\boldsymbol{\varphi}+k_z\frac{\Delta z}{2}\mathbf{z}-\omega\frac{\Delta t}{2}\tau))}\right]. \tag{15}$$

where k_r, n, k_z are the r, φ, z components of the numerical wavevector and ω is the wave angular frequency, r is a radial coordinate. The solutions for the magnetic field components and currents have a similar form as (15). Substituting the wave expression of (15) into the finite-difference set of equations of (6)-(8) yields after simplification the following set of equations:

$$\frac{1}{r\Delta\varphi}\cot\left(k_z\frac{\Delta z}{2}\right)\tan\left(n\frac{\Delta\varphi}{2}\right)E_z - \frac{1}{\Delta z}E_\varphi =$$
$$\frac{1}{\Delta t}\frac{\sin\left(\omega\frac{\Delta t}{2}\right)}{\cos\left(n\frac{\Delta\varphi}{2}\right)\sin\left(k_z\frac{\Delta z}{2}\right)}H_r, \tag{16}$$

$$\frac{1}{\Delta z}\cot\left(k_r\frac{\Delta r}{2}\right)\tan\left(k_z\frac{\Delta z}{2}\right)E_r - \frac{1}{\Delta r}E_z =$$
$$\frac{1}{\Delta t}\frac{\sin\left(\omega\frac{\Delta t}{2}\right)}{\sin\left(k_r\frac{\Delta r}{2}\right)\cos\left(k_z\frac{\Delta z}{2}\right)}H_\varphi, \tag{17}$$

$$\left[\frac{2}{\Delta r}\sin\left(k_r\frac{\Delta r}{2}\right) - \frac{j}{r}\cos\left(k_r\frac{\Delta r}{2}\right)\right]\cot\left(n\frac{\Delta\varphi}{2}\right)E_\varphi-$$
$$\frac{2}{r\Delta\varphi}\cos\left(k_r\frac{\Delta r}{2}\right)E_r = \frac{2}{\Delta t}\frac{\sin\left(\omega\frac{\Delta t}{2}\right)}{\sin\left(n\frac{\Delta\varphi}{2}\right)}H_z, \tag{18}$$

$$\frac{2}{r\Delta\varphi}\sin\left(n\frac{\Delta\varphi}{2}\right)H_z - \frac{2}{\Delta z}\sin\left(k_z\frac{\Delta z}{2}\right)H_\varphi =$$
$$-\frac{2}{\Delta t}\frac{\sin\left(\omega\frac{\Delta t}{2}\right)}{\cos\left(k_r\frac{\Delta r}{2}\right)}E_r - j\frac{\cos\left(\omega\frac{\Delta t}{2}\right)}{\cos\left(k_r\frac{\Delta r}{2}\right)}J_r, \tag{19}$$

$$\frac{2}{\Delta z}\sin\left(k_z\frac{\Delta z}{2}\right)H_r - \frac{2}{\Delta r}\sin\left(k_r\frac{\Delta r}{2}\right)H_z =$$
$$-\frac{2}{\Delta t}\frac{\sin\left(\omega\frac{\Delta t}{2}\right)}{\cos\left(n\frac{\Delta\varphi}{2}\right)}E_\varphi - j\frac{\cos\left(\omega\frac{\Delta t}{2}\right)}{\cos\left(n\frac{\Delta\varphi}{2}\right)}J_\varphi, \tag{20}$$

$$\left[\frac{2}{\Delta r}\sin\left(k_r\frac{\Delta r}{2}\right) - \frac{j}{r}\cos\left(k_r\frac{\Delta r}{2}\right)\right]H_\varphi-$$
$$\frac{2}{r\Delta\varphi}\sin\left(n\frac{\Delta\varphi}{2}\right)H_r =$$
$$-\frac{2}{\Delta t}\frac{\sin\left(\omega\frac{\Delta t}{2}\right)}{\cos\left(k_z\frac{\Delta\varphi}{2}\right)}E_z - j\frac{\cos\left(\omega\frac{\Delta t}{2}\right)}{\cos\left(k_z\frac{\Delta z}{2}\right)}J_z, \tag{21}$$

$$-\frac{2j}{\Delta t}J_r\tan\left(\omega\frac{\Delta t}{2}\right) + \vartheta_s J_r = \omega_{ps}^2 E_r + \left(J_\varphi\Omega_z - J_z\Omega_\varphi\right), \tag{22}$$

$$-\frac{2j}{\Delta t}J_\varphi\tan\left(\omega\frac{\Delta t}{2}\right) + \vartheta_s J_\varphi = \omega_{ps}^2 E_\varphi + \left(J_z\Omega_r - J_r\Omega_z\right), \tag{23}$$

$$-\frac{2j}{\Delta t}J_z \tan\left(\omega\frac{\Delta t}{2}\right) + \vartheta_s J_z = \omega_{ps}^2 E_z + (J_r\Omega_\varphi - J_\varphi\Omega_r). \quad (24)$$

The set of equations (16)-(24) still depends on r and no solution exists which holds for all r. However, if r is sufficiently large, the r-dependent terms become negligible. Let us illustrate under which condition the cylindrical dispersion relation approximates the dispersion realtion in the Cartesian coordinate system. Assuming the solutions of the wave fields and currents in a form

$$\frac{1}{2}\left[e^{(j(k_x\frac{\Delta x}{2}\mathbf{x}+k_y\frac{\Delta y}{2}\boldsymbol{y}+k_z\frac{\Delta z}{2}\mathbf{z}-\omega\frac{\Delta t}{2}\tau))}+\right.$$
$$\left. + e^{(-j(k_x\frac{\Delta x}{2}\mathbf{x}+k_y\frac{\Delta y}{2}\boldsymbol{y}+k_z\frac{\Delta z}{2}\mathbf{z}-\omega\frac{\Delta t}{2}\tau))}\right] \quad (25)$$

and applying the same set of procedures mentioned above, it can be seen that the discretized dispersion matrix in the cylindrical coordinate system repeats the matrix in the Cartesian coordinate system under the following condition (see first terms in the equations (18) and (21))

$$\frac{2}{\Delta r}sin(k_r\frac{\Delta r}{2}) >> \frac{cos(k_r\frac{\Delta r}{2})}{r}, \quad (26)$$

which means that if the wavelength is significantly shorter than the distance from the point of consideration to the cylindrical axis, i.e $k_r >> 1/r$ (where r is a distance from the point of consideration to the cylindrical axis), the cylindrical dispersion relation approximates the cartesian one.

Only under (26) setting the determinant of (16-24) to zero we obtain the expression for the full discrete dispersion relation (27), valid for phenomena which occur far away from the central axis of the cylindrical coordinate system. The expression for the 3D discrete dispersion relation is:

$$\begin{aligned}
&\left[a_1^2 a_2^2 b_3^2 \epsilon_1 + a_1^2 a_3^2 b_2^2 \epsilon_3 + a_2^2 a_3^2 b_1^2 \epsilon_1\right]\tilde{k}^2 - \\
&\left[a_1^2(b_2^2+b_3^2)\epsilon_1\epsilon_3 + a_2^2(b_1^2+b_3^2)(\epsilon_1^2-\epsilon_2^2) + \right. \\
&\left. a_3^2(b_1^2+b_2^2)\epsilon_1\epsilon_3\right]b_4^2 + \epsilon_3(\epsilon_1^2-\epsilon_2^2)b_4^4 = 0.
\end{aligned} \quad (27)$$

where

$$\epsilon_1 = 1 - \sum_s \frac{\omega_{ps}^2\tilde{\omega}}{\omega^*(\tilde{\omega}^2 - \Omega_s^2)},$$

$$\epsilon_2 = -\sum_s \frac{\omega_{ps}^2\Omega_s}{\omega^*(\tilde{\omega}^2 - \Omega_s^2)},$$

$$\epsilon_3 = 1 - \sum_s \frac{\omega_{ps}^2}{\omega^*\tilde{\omega}},$$

with

$$\omega^* = \frac{2}{\Delta t}tan(\omega\frac{\Delta t}{2}),$$

$$\tilde{\omega} = \omega^* + i\nu_s,$$

and $\tilde{k}^2 \equiv b_1^2 + b_2^2 + b_3^2$ is the square of the discretized wave vector.

To simplify the equation the following notations are used:

$$a_1 \equiv cos(k_r\frac{\Delta r}{2}), \quad b_1 \equiv \frac{2}{\Delta r}sin(k_r\frac{\Delta r}{2}),$$

$$a_2 \equiv cos(n\frac{\Delta\varphi}{2}), \quad b_2 \equiv \frac{2}{r\Delta\varphi}sin(n\frac{\Delta\varphi}{2}),$$

$$a_3 \equiv cos(k_z\frac{\Delta z}{2}), \quad b_3 \equiv \frac{2}{\Delta z}sin(k_z\frac{\Delta z}{2}),$$

$$a_4 \equiv cos(\omega\frac{\Delta t}{2}), \quad b_4 \equiv \frac{2}{c\Delta t}sin(\omega\frac{\Delta t}{2}), \quad (28)$$

Below the behavior of the dispersion relation for a number of specific scenarios will be studied.

A. Vacuum case

For vacuum, when the plasma density is zero, the discrete dispersion relation (27) is:

$$\left[a_1^2 a_2^2 b_3^2 + a_1^2 a_3^2 b_2^2 + a_2^2 a_3^2 b_1^2\right]\tilde{k}^2$$
$$- \left[a_1^2(b_2^2+b_3^2) + a_2^2(b_1^2+b_3^2) + a_3^2(b_1^2+b_2^2)\right]b_4^2 + b_4^4 = 0. \quad (29)$$

Ensuring that the problem is well-resolved (Δr, $\Delta\varphi$, $\Delta z << \lambda$) and using the Taylor series expansion of the sine and cosine for a small parameter, a_1, a_2, a_3 are 1 to first order, and we obtain the vacuum dispersion relation:

$$k_r^2 + (\frac{k_\varphi}{r})^2 + k_z^2 \equiv k^2 = \frac{\omega^2}{c^2}. \quad (30)$$

Demanding that real k always map to real ω leads to the Courant condition:

$$c\Delta t < \frac{1}{\sqrt{(\frac{1}{\Delta r})^2 + (\frac{1}{r\Delta\varphi})^2 + (\frac{1}{\Delta z})^2}}. \quad (31)$$

Eq. (30) is a well-known dispersion relation for electromagnetic waves in vacuum, when the frequency is proportional to the wavenumber [28, 29].

B. Nonmagnetized plasma

In the absence of a background magnetic field, the term ϵ_1 in equation (27) becomes equal to the term ϵ_3, and the term ϵ_2 is zero. The full discrete dispersion relation (27) reduces to:

$$\left[a_1^2 a_2^2 b_3^2 + a_1^2 a_3^2 b_2^2 + a_2^2 a_3^2 b_1^2\right]\epsilon_3\tilde{k}^2$$
$$- \left[a_1^2(b_2^2+b_3^2) + a_2^2(b_1^2+b_3^2) + a_3^2(b_1^2+b_2^2)\right]\epsilon_3^2 b_4^2 \quad (32)$$
$$+ \epsilon_3^3 b_4^4 = 0.$$

Neglecting second order terms of the Taylor series expansion gives a_1, a_2, a_3 equal to 1, b_1, b_2, b_3 becomes k_r, n/r, k_z, respectively and b_4 turns into $\frac{\omega}{c}$. After simplification (32) reduces to

$$\epsilon_3\left(\tilde{k}^2 - \epsilon_3\frac{\omega^2}{c^2}\right)^2 = 0 \quad (33)$$

Finally, the nonmagnetized plasma dispersion relation (32) takes a form

$$\tilde{k}^2 = \epsilon_3 b_4^2. \tag{34}$$

If the collisional frequency term is neglected, $\tilde{\omega}$ becomes equal to ω^* and ϵ_3 takes a form

$$\epsilon_3 = 1 - \left(\frac{\Delta t}{2}\right)^2 \cot^2\left(\frac{\omega \Delta t}{2}\right) \sum_s \omega_{ps}^2. \tag{35}$$

Now Eq.(34) can be resolved for $sin(\omega \Delta t/2)$:

$$\tilde{k}^2 = \left(\frac{2}{c\Delta t}\right)^2 \sin^2(\omega \frac{\Delta t}{2}) - \frac{1}{c^2} \cos^2(\omega \frac{\Delta t}{2}) \sum_s \omega_{ps}^2. \tag{36}$$

Here, only the terms of the first order of the Taylor series expansion are retained, and we obtain the slow wave dispersion relation [31]:

$$k^2 = \frac{\omega^2}{c^2} \left(1 - \sum_s \frac{\omega_{ps}^2}{\omega^2}\right) = \epsilon_3 \frac{\omega^2}{c^2}. \tag{37}$$

Analysis of the Eq. (36) shows that the Courant condition for a nonmagnetized plasma is completely equivalent to the vacuum Courant condition (31).

C. Magnetized plasma

1) 3D: Eq. 27 represents the general form of the numerical dispersion relation in a full three-dimensional case.

2) 2D: Neglecting the terms of second order of the Taylor series expansion in the grid step, Eq. (27) becomes:

$$\left[(b_1^2 + b_3^2)\epsilon_1 + b_2^2\epsilon_3\right]\tilde{k}^2$$
$$- \left[(b_1^2 + 2b_2^2 + b_3^2)\epsilon_1\epsilon_3 + (b_1^2 + b_3^2)(\epsilon_1^2 - \epsilon_2^2)\right]b_4^2 \tag{38}$$
$$+\epsilon_3\left[\epsilon_1^2 - \epsilon_2^2\right]b_4^4 = 0.$$

When the problem is uniform along the z- direction ($b_3 = 0$), the magnetized dispersion relation (38) becomes:

$$\left[b_1^2\epsilon_1 + b_2^2\epsilon_3\right]\tilde{k}^2$$
$$- \left[(b_1^2 + 2b_2^2)\epsilon_1\epsilon_3 + b_1^2(\epsilon_1^2 - \epsilon_2^2)\right]b_4^2 \tag{39}$$
$$+\epsilon_3\left[\epsilon_1^2 - \epsilon_2^2\right]b_4^4 = 0.$$

3) 1D: When the problem is uniform along z- and $\varphi-$ directions $b_2 = b_3 = 0$ and the wave is transverse, Eq. (39) can be further simplified to:

$$\epsilon_1\tilde{k}^4 - \left[\epsilon_1\epsilon_3 + (\epsilon_1^2 - \epsilon_2^2)\right]b_4^2\tilde{k}^2$$
$$+\epsilon_3\left[\epsilon_1^2 - \epsilon_2^2\right]b_4^4 = 0. \tag{40}$$

Eq. (40) gives two well-known solutions. One of them is the slow wave dispersion relation (34) $\tilde{k}^2 = \epsilon_3 b_4^2$ and the second one is:

$$\tilde{k}^2 = \frac{\epsilon_1^2 - \epsilon_2^2}{\epsilon_1} b_4^2 = \alpha b_4^2. \tag{41}$$

Keeping the terms of the first order of the Taylor series expansion, Eq. (41) gives the dispersion relation of the extraordinary wave [31]:

$$k^2 = \frac{\epsilon_1^2 - \epsilon_2^2}{\epsilon_1} \frac{\omega^2}{c^2} = \alpha \frac{\omega^2}{c^2}. \tag{42}$$

IV. ACCURACY ANALYSIS

Before employing this numerical algorithm, we need to determine if it is applicable to the problems at hand. Tackling any problem numerically (rather than analytically) inevitably introduces discretisation errors. The study of a numerical algorithm's accuracy involves studying, and imposing, bounds on these errors. An analysis of the discretisation error can be performed by comparing numerical and exact dispersion relations, as in [12], [17], [32], [36]. The approach followed by [12] is based on comparing the numerically calculated dispersion which expresses how the index of refraction depends on the wave frequency with the analytically predicted dispersion. Subsequently the numerical errors are calculated as the deviation of the numerical results of the corresponding values obtained analytically. However, rather than using the relative error on the dispersion (as Cummer did) we propose to use the relative dispersion error defined as :

$$\delta = |Re\left(N_{num} - N_{anal}\right)/Re\left(N_{anal}\right)|, \tag{43}$$

where N_{num} and N_{anal} are the numerically and analytically obtained indexes of refraction.

In order to evaluate the relative dispersion error we choose to investigate the dispersion relation of the extraordinary wave (41). This particular plasma mode is selected because the range of the propagation of this wave contains ion-cyclotron frequencies, in the frequency range of which the RF antennas of the tokamaks operate. The numerical tests were conducted in the frequency range from 0 to the low hybrid frequency (ω_{LH}), because exactly in this range the values of the wave vector are real and the wave itself propagates through the simulation region (see Fig.2). The considered time-steps lie
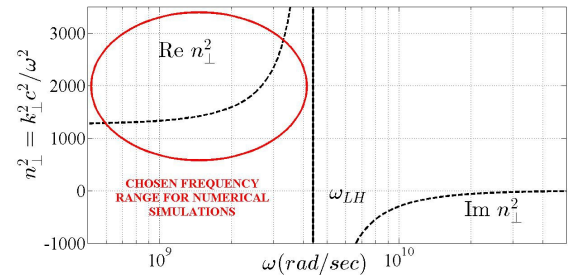
Fig. 2. Analytical dispersion relation of the extraordinary wave. The dispersion relation of the extraordinary wave is specifically selected for numerical simulations because the range of the propagation contains the ion-cyclotron frequencies (on which the RF antennas of the tokamaks work). The frequency range from 0 to ω_{LH} marked in red is chosen for numerical simulations because in this range the values of the wave vector are real and the wave itself propagates through the simulation period.

in an interval from 0 to π/ω. The numerical simulations are conducted in the collisionless homogeneous media with initial

plasma parameters $n_e = n_D = 10^{19} \ (1/m^3)$ and background magnetic field B_0 equal to $3 (T)$.

On Fig. 3 the contour plot shows the relative dispersion error (see Eq. (43)), as a function of frequency ω and time-step Δt. The contour lines (of this contour plot) demarcate the borders

Fig. 3. A contour plot of the dispersion error as a function of ω and Δt. The lines of the contour plot demarcate the borders of the areas with certain accuracy. The Courant limit (red solid line) shows the border between stable and unstable simulation areas.

of the areas in the $(\omega, \Delta t)$ plane where the relative dispersion error is below a certain numerical value of the dispersion error. This will give us guidance on how to choose Δt for a certain frequency range provided that we require a certain accuracy. For example, if the values of the frequency and time-step are chosen within the area demarcated by the contour labeled "0.01", it is guaranteed that the dispersion error will not exceed 1 %. The conclusion from the discussion is that in order to get a sufficient accuracy (i.e. an relative dispersion error of less than, e.g. 1%) the time-step has to be chosen such that the point $(\omega, \Delta t)$ lies in an area demarcated by the right contours illustrated in Fig. 3.

V. STABILITY

One of the standard analytical approaches to examine the stability of a numerical technique is a method developed by von Neumann [2]. This method expresses the numerical error introduced at any discrete time instant as a spatial Fourier series (over a bounded space). Numerical stability is guaranteed if the magnitude of every Fourier coefficient attenuates over one time-step (i.e., if every Fourier coefficient is multiplied by a number with magnitude smaller than or equal to 1 at each time-step). Under this condition, assuming, that each Fourier coefficient is initially bounded, each coefficient remains bounded at all subsequent time-steps. Since the system is linear, the total error after N time steps, which is represented by the sum of the Fourier series associated with the errors introduced at the N past time-steps, is also bounded at any time-step. Since the original von Neumann analysis relies on Fourier series, its applicability is restricted because of the restriction to cases with periodic boundary conditions. However, these original von Neumann approach can be extended to much wider circumstances (with much broader applicability). This extended version of the von Neumann approach suits our needs, as we are concerned with the stability of the applied method independent of boundary conditions.

Even though the analytical application of the von Neumann method is rather complicated in case of magnetized plasma, it is possible to apply this technique for the numerical analysis.

The 1D problem with the wave propagating in the r-direction with non-zero components $E_r, E_z, H_\varphi, J_r, J_z$ in magnetized plasma is considered. The difference equations can be written in the general form:

$$\underbrace{F^{t+1}}_{future} = M \underbrace{F^t}_{past}, \qquad (44)$$

where F represents a column vector containing all discretized electric, magnetic and current field components and with M is the amplification matrix. The numerical scheme is stable if the eigenvalues of M lie on the unit circle in the complex plane. Only when there are losses either due to the nature of the material or due to radiation escaping from the simulation region, some of the eigenvalues may fall inside the unit circle [9].

In Fig. 4 the eigenvalues of the amplification matrix of the applied FDTD method for magnetized plasma are presented.

In this particular case the simulation parameters are: $n_{e-} = 3 \cdot 10^{19} \ (1/m^3)$, $n_D = 0.98 n_{e-} \ (1/m^3)$, $n_H = 0.02 n_{e-} \ (1/m^3)$. The background magnetic field is uniform and it is equal to 3 T. The space step Δr is calculated based on the analytical dispersion relation [30], [31]. The time-step Δt is determined in an agreement with the Courant stability condition [2]. This numerical analysis shows that the

Fig. 4. Numerical stability test. The eigenvalues of the amplification matrix 44 are located on a unit circle in the complex plane. The initial simulation parameters are: $n_{e-} = 3 \cdot 10^{19} \ (1/m^3)$, $n_D = 0.98 n_{e-} \ (1/m^3)$, $n_H = 0.02 n_{e-} \ (1/m^3)$. The background magnetic field is uniform and it is equal to 3 T.

developed technique is indeed stable at these parameters. In particular, we find that the time-step has to be sufficiently small, i.e. it must satisfy the vacuum Courant condition. If it exceeds the Courant limit, instability would occur [16].

VI. BOUNDARY CONDITION

In this Section we give the description of the necessary boundary conditions for the computational domain. The boundary conditions were developed to describe two important phenomena. First one has to model the power source that

launches the wave into the plasma. Another one has to deal with the wave fields at the plasma edges.

As a power source we use a so-called hard source [28] or a "point" source, which in our cylindrical case is really an infinitely thin cylindrical surface along the toroidal direction carrying a constant amplitude current with sinusoidal time-dependence at a particular frequency ω. It is switched on at $t = 0$ and flows until regime conditions are met. In more detail, the wave electric field is defined at a surface $r_a - N_{cells} = const$ which models as it is mentioned above the Radio Frequency (RF) antenna or a power source condition (PSC) in the tokamak. Here, N_{cells} is the number of cells. Among the waves that are possibly exited by the hard source we choose to investigate only the wave mode that is used for plasma heating in the tokamak, i.e. only the mode that propagates towards the cylindrical axis.

In the presented study the RF antenna is unrestricted in $\varphi-$ and z-directions to exclude the antenna edge effects on the wave propagation. The external confined magnetic field (uniform or nonuniform) is oriented along the φ-direction. The ordinary wave (the electric field is parallel to the external magnetic field) is launched by the PSC $E_\varphi = E_0 sin(\omega t)$. The extraordinary wave (the electric field is perpendicular to the external magnetic field) is launched by the PSC $E_z = E_0 sin(\omega t)$. Plasma media occupies the space of $[r_b, r_a]$ in r-direction, where $r_a - r_b$ is the width of the plasma column.

One of the types of the applied boundary conditions is the Perfect Electric Conductor (PEC). Thus, the wave reaching the surface $r_b = const$ is reflected completely back to the antenna. Since at $r_a = const$ the PSC plays the role of PEC for the reflected waves, we expect a process of multireflection between the surfaces $r_a = const$ and $r_b = const$. We would like to note that the multireflection process might evoke the unrestrained growth of the electromagnetic field amplitude and under these circumstances the steady state condition cannot be reached. However, including of the collision frequency term ϑ_s (Eq. (3)) will cause the wave dissipation which allows the steady state to be reached. The magnitude of the collision frequency term defines the time needed to reach the steady state. Note, that there is a restriction on the collision frequency term value. It has to be large enough to minimize the wave reflection from the boundary r_b back to the antenna. In Section VII such estimations of the collisional term values will be given. The general frame of the boundary technique is illustrated on Fig. 5 together with the direction of the wave propagation and the location of the antenna.

VII. NUMERICAL EXAMPLES

A. Numerical Validation

Above we have proven that the dispersion relation of the actual problem and its fully discretized FDTD counterpart will become identical for sufficiently small time and space steps. This claim is further substantiated by providing numerical data from our own cylindrical FDTD code. In Fig. 6-7 the discretized dispersion relation of the extraordinary (42) and ordinary (37) waves are compared to the analytical ones. The numerical results are obtained for the one-dimensional
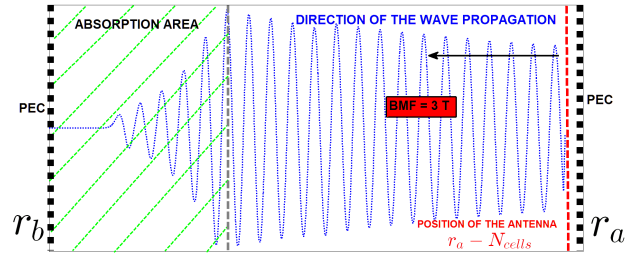

Fig. 5. Illustration of the simulation structure. Perfect Electric Conductor used as boundary conditions. The power source is located significantly close to the right edge of the simulation domain. The damping boundary condition is set at the distance that would allow to provide the effective damping.

cylindrical case (the model is invariant in φ and z direction). We consider a one-ion (deuterium) homogeneous collisionless plasma with the following initial parameters: the density is $n_e = n_{De} = 3 \cdot 10^{19} (1/m^3)$, the uniform background magnetic field B_0 is equal to 3 (T), the lower hybrid frequency is $\omega_{LH} = 3.79 \cdot 10^9$ (rad/sec), the source frequency is equal to $\omega = 2.87 \cdot 10^8$ (rad/sec).
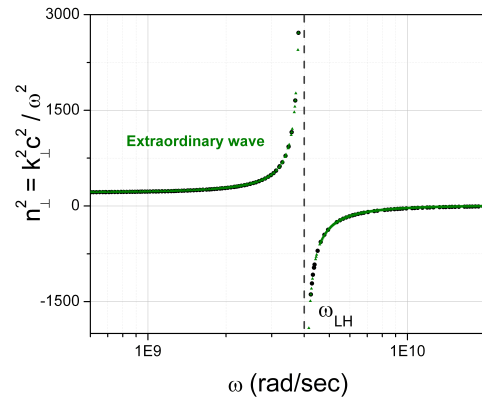

Fig. 6. Analytical and the numerical dispersion curves of the extraordinary wave in a low frequency range for 1D collisionless toroidal plasma. ($n_e = n_{De} = 3 \cdot 10^{19} (1/m^3)$, $B_0 = 3(T)$). Theoretical data: black dots; numerical data: green dots.

The presented graphs show that the numerical results are in very good agreement with the theory.

B. Curvature Effects

The typical geometry of the JET tokamak and its plasma parameters will be used to carry out some of the numerical tests. The RF antenna is located at $r_a = 4$ (m). The diameter of the plasma column is 2 m therefore $r_b = 2$ (m). In order to simplify the numerical tests we assume that the magnetic field is uniform and it is equal to 3 (T). The antenna launches the Fast Wave (FW) ([30], [31]) with a source frequency f that is equal to 45.7 (MHz). The corresponding angular frequency ω is $2.87 \cdot 10^8$ (rad/sec). The ion- and electron density in the plasma is $3 \cdot 10^{19}$ (m^{-3}).
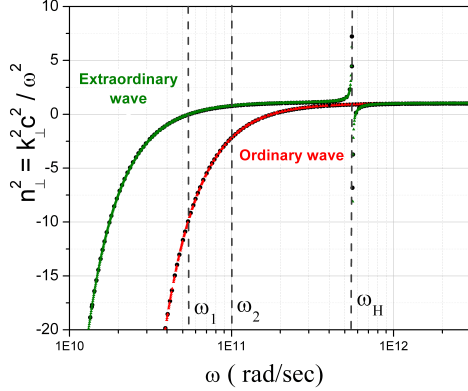
Fig. 7. Analytical and the numerical dispersion curves waves in the high frequency range in the cylindrical geometry. The initial conditions are the same as on Fig. 6. Theoretical data: black dots; numerical data: green dots stand for extraordinary wave, red dots- ordinary wave.

Fig. (8) shows the comparison of the field structures in the Cartesian (red dotted solid line) and the cylindrical (black dotted solid line) coordinate systems. The figures show the steady state distribution of the wave fields.
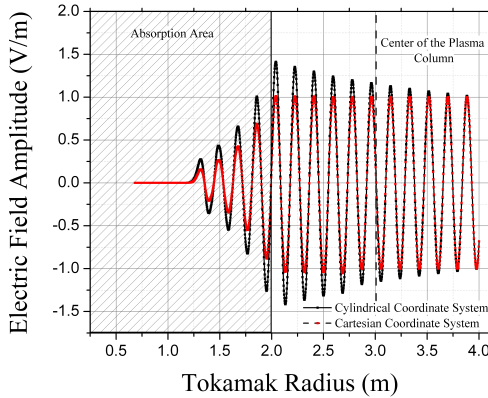

Fig. 8. Curvature effects for the electric field (E_z- component) structures in the Cartesian (black solid dotted line) and in the cylindrical (red dotted dashed line) coordinate systems. The shaded light grey area is the absorption area which is responsible for providing damping of electromagentic waves. The collision frequency term is equal to $\omega/2\pi$, where ω is $2.87 \cdot 10^8$ (rad/sec). The amplitude of the electric field in the Cartesian coordinate system stays constant during the whole simulation period. The amplitude of the electric field in the cylindrical coordinate system grows in $\sqrt{2}$ times.

The amplitude of the wave field is constant in a plasma column in the Cartesian coordinate system. Using the definition of the energy flux density, i.e. Poynting vector $\mathbf{S} = [\mathbf{E} \times \mathbf{B}]$, the growth of the amplitude in the cylindrical coordinate system may be estimated. For example, we propose to compare the magnitude of the time- averaged Poytning flux at two different positions: at $r_a = 4$ (m) and at $r_b = 2$ (m), which gives us

$$S_1 r_a = S_2 r_b \qquad (45)$$

that leads to $S_2 = \frac{r_a}{r_b} S_1$. Since for sinusoidal electromagnetic

plane waves the time-averaged Poytnign flux S is equal to E_0^2 (E_0 is the amplitude of the electric field), the amplitude of the electromagnetic wave grows in $\sqrt{\frac{r_a}{r_b}}$ times, which means that in our case it grows in $\sqrt{2}$ times and as it can be seen on a Fig. 8, the numerical results are in a good agreement with theoretical predictions.

C. Collision Frequency Term Effect

Here, the approximate analysis will be carried out to estimate the effect of the collision frequency term in Eq. (3). In order to simplify the estimation the analysis will be done in the Cartesian coordinate system.

The fast wave propagates to the boundary $x = r_b$ according to the law $E_y(x) = E_0 exp(jk_x x)$, where E_0 is the wave amplitude defined by the antenna and k_x is x-component of the FW wave vector which is defined by the FW dispersion relation [31]. Reaching the boundary $x = r_b$ the FW is partially reflected with coefficient R and partially transmitted with coefficient T. Hence, the wave field in the range $[r_b, r_a]$ is defined as $E_y(x) = E_0(exp(jk_x x) + Rexp(-jk_x x))$. The wave field behind the boundary $x = r_b$ is defined by $E_y(x) = E_0 T exp(jk_x' x)$, where k_x' stands for the FW wave vector in a plasma media with collisions. The well-known relation between the electric and magnetic fields of the FW is $\frac{\partial H_z}{\partial t} = -\frac{\partial E_y}{\partial x}$ (the problem is uniform along the y direction). Since the tangential components of the electromagnetic field have to be continues at the boundary $x = r_b$ it provides two equations:

$$1 + R = T, \qquad (46)$$

$$k_x(1 - R) = k_x' T. \qquad (47)$$

These equations can be resolved for the transmission R and reflection T coefficients, respectively:

$$T = \frac{2}{1 + k_x'/k_x}, \qquad (48)$$

$$R = T - 1. \qquad (49)$$

Since the time- averaged Poyting flux for plane waves is proportional to the square of the wave field amplitudes the coefficient of the power transfer through the boundary is equal to $|T|^2$ and the coefficient of power reflection from the boundary is $1 - |T|^2$. In Fig. 9 the power reflection coefficient is calculated in the Cartesian coordinate system. It is compared with the penetration depth of the FW behind the boundary $x = r_b$ (it is defined from $Im(k_x')$). The power reflection does not even reach 7% when the collisional frequency is equal to the antenna frequency. However, the wave penetration depth in this case is only 0.0641 (m) which does not allow the wave to reach the axis. The analysis shows that even $\nu_s = 0.1\omega$ with a power reflection of 0.1% is already enough for efficient damping of the electromagnetic wave.
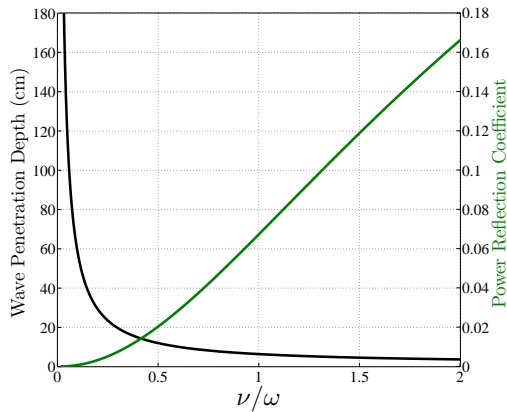
Fig. 9. The dependence of the absolute value of the reflection coefficient R on the normalized value of the collisional frequency. The power reflection coefficient (green solid line) is compared to the wave penetration depth in cm (black solid line). It can be seen that even with the collision frequency term ν_s equal to 0.1ω the efficient damping of the electromagnetic wave is guaranteed.

VIII. CONCLUSIONS

The FDTD method has been applied to describe the electromagnetic wave propagation through fusion plasmas in the cylindrical geometry. The hybrid scheme of [14] with both the explicit part (leapfrog electric/magnetic interaction) and implicit part (electric/current interactions) was implemented due to better numerical stability than the fully explicit approaches [17]. A similar approach to our applied numerical scheme is used in [15]. However, the method in [15] is developed in the Cartesian coordinate system. Moreover, the electric field and current components in the Yee cell are positioned differently which leads to the different way of solving the obtained set of equations. In this paper, the 3D full discrete dispersion relation has been obtained and compared with the analytical solution. The numerical stability criterion has been investigated analytically for nonmagnetized uniform plasma, and numerically for magnetized plasma, and it was found to be identical to the vacuum Courant limit. The developed boundary conditions allow to reach a steady state of the electromagnetic field distribution even when the antenna continuously launches the power to the plasma. The numerical examples are provided to show that the developed algorithm based on the hybrid FDTD method performs properly and the dispersive behavior of the different plasma modes are predicted correctly.

REFERENCES

[1] K. Yee, " A numerical solution of initial boundary value problems involving Maxwell's equations in isotropic media," *IEEE Trans. Antennas Propag.*, vol. 14, pp. 302- 307, 1966.

[2] A. Taflove and S. C. Hagness, *Computational Electromagnetics: Finite-Difference Time-Domain Method*, 3rd. ed. Norwood, MA: Artech House, 2005.

[3] R. J. Luebbers, F. Hunsberger, and K. S. Kunz, " A frequency- dependent finite- difference time- domain formulation for transient propagation in a plasma", *IEEE Trans. Antennas Propag.*, vol.39, pp. 29-34, Jan. 1991.

[4] D. F. Kelley and R. J. Luebbers "Piecewise linear recursive convolution for dispersive media using FDTD", *IEEE Trans. Antennas Propag.*, vol. 44, pp. 792- 797, June 1996.

[5] R. Siushansian and J. LoVetri, "A comparison of numerical techniques for modeling electromagnetic dispersive media", *IEEE Microwave Guided Wave Lett.*, vol. 5, pp. 426- 428, Dec. 1995.

[6] R. J. Luebbers, F. Hunsberger, K. S. Kunz, R. Standler, and M. Sneider, "A frequency- dependent finite- difference time- domain formulation for dispersive materials", *IEEE Trans. Electromagn. Compat.*, vol. 32, pp. 222- 227, Aug. 1990.

[7] R. J. Luebbers and F. Hunsberger, "FDTD for Nth- order dispersive media", *IEEE Trans. Antennas Propag.*, vol. 40, pp. 1297- 1301, 1992.

[8] L. J. Nickisch and P. M. Franke, "Finite- difference time- domain solution of Maxwell's equations for the dispersive ionosphere", *IEEE Antennas Propag. Mag.*, vol. 34, pp. 33- 39, Oct. 1992.

[9] D. M. Sullivan, "Z- trasform theory and the FDTD method", *IEEE Trans. Antennas Propagat.*, vol. 44, pp. 28- 34, Jan. 1996.

[10] T. Kashiwa, N. Yoshida and I. Fukai, "Transient analysis of a magnetized plasma in three- dimensional space", IEEE Trans. Antennas Propag., vol. 36, pp. 1096- 1105, Aug. 1988.

[11] G. Singh, E. L. Tan, and Z. N. Chen, "A split-step FDTD method for 3- D Maxwell's equations in general anisotropic media", *IEEE Trans. Antennas Propag.*, vol. 58, pp. 3647- 3657, Nov. 2010.

[12] S. A. Cummer, "An analysis of new and existing FDTD methods for isotropic cold plasma and a method for improving their accuracy", *IEEE Tras. Antennas Propag.*, vol. 45, pp. 392- 400, 1997.

[13] J. L. Young and R. O. Nelson, "A summary and systematic analysis of FDTD algorithms for linearly dispersive media", *IEEE Antennas and Propagation Magazine*, vol. 43, No 1, February 2001.

[14] D. N. Smithe, " Finite- difference time- domain simulation of fusion plasmas ar radiofrequency time scales", Phys. Plasma 14,056104, 2007.

[15] Y. Yu and J. J. Simpson, "An E-J Collocated 3- D FDTD Model of Electromagnetic Wave Propagation in Magnetized Cold Plasma", *IEEE Trans. Antennas Propag.*, vol. 58, No. 2, pp. 469-478, February 2010.

[16] W. Tierens and D. De Zutter, "An unconditionally stable time- domain discretization on cartesian meshes for the simulation of nonuniform magnetized cold plasma", *Journal of Computational Physics*, vol. 231, pp. 5144- 5166, 2012.

[17] J. L. Young, "A full finite difference time domain implementation for radio wave propagation in a plasma", *Radio Sci.*, vol. 29, pp. 1513- 1522, 1994.

[18] G. Mur, "Absorbing Boundary Conditions for the Finite- Difference Approximation of the Time- Domain Electromagnetic- Field Equations", IEEE Transactions on Electromagnetic Compatibility, vol. EMC-23, No. 4, pp.377-382, 1981.

[19] J.-P. Berenger, "A Perfectly Matched Layer for the Absorption of Electromagnetic Waves", Journal of Computational Physics, vol.114, pp.185-200, 1994.

[20] Y. Yu, J.J. Simpson, "A Magnetic Field- Independent Absorbing Boundary Condition for Magnetized Cold Plasma", IEEE Antennas and Wireless Propagation Letters, vol.10, pp.294-297, 2011.

[21] W. Tierens and D. De Zutter, "Finite-temperature corrections to the time-domain equations of motion for perpendicular propagation in nonuniform magnetized plasmas", Physics of Plasmas, 2012

[22] W. Tierens and D. De Zutter, "Stable time-domain differential equations which reproduce the warm plasma dielectric tensor" 20th Topical Conference on Radio Frequency Power in Plasmas, 2013

[23] F. Zheng, Z. Chen, J. Zhang, "A Fifnite- Difference Time- Domain Method Without the Courant Stability Conditions", IEEE Microwave and Guided Letters, vol. 9, No. 11, pp. 441- 443, 1999.

[24] J.P. Boyd, "Chebyshev and Fourier Spectral Methods", Dover, New York, 2001.

[25] N. Dib, T. Weller, and M. Scardelletti, "Analysis of 3-D cylindrical structures using the finite difference time domain method", IEEE Trans. on MMT, pp. 925-927.

[26] F. Akleman, L. Sevgi, "Comparison of retangular and cylindrical FDTD representations on a ring resonator problem", Turk J Elec Engin, vol. 16, No. 1, 2008.

[27] A. Trakic, H. Wnag, F. Hiu, H. S. Lopez, S. Crozier, "Cylindrical 3 D FDTD algorithm for the computation of low frequency transient eddy currents in MRI", *Proc. Intl. Soc. Mag. Reson. Med.*,vol. 14, 2006.

[28] F. Costen and J. P. Berenger,"Comparison of FDTD hard source with FDTD soft source and accuracy assessment in Debye media", *IEEE Trans. Antennas and Propag.*, vol. 57, pp. 2014-2022, 2009.

[29] N. A. Krall and A. W. Trivelpiece, "Principles of plasma physics", New York, 1973.

[30] T. H. Stix,"Waves in plasma", New York, 1992.

[31] M. Brambilla, "Kinetic theory of plasma waves", Oxford University Press, 1998.

[32] P. Petropolous "Stability and phase error analysis of FDtD in dispersive dielectrics", *IEEE Trans. Antennas Propag.*, vol. 42, pp. 62- 69, 1994.

[33] R. Richtmyer and K. Morton, "Difference methods for initial- value problems", New York: Wiley, 1967.

[34] T. Woo, S. Hagness, "Pseudospectral time- domain methods for modeling optical wave propagation in second- order nonlinear materials", J. Opt. Soc. Am. B, vol. 21, No. 2, February, 2004.

[35] D. M. Sullivan, "Electromagnetic simulation using the FDTD method", IEEE press series on RF and microwave technology, New York, 2000.

[36] J. H. Lee and D. K. Kalluri, "Three- Dimensional FDTD Simulation of Electromagnetic Wave Transformation in a Dynamic Inhomogeneous Magnetized Plasma", *IEEE Trans. Antennas Propag.*, vol. 47, pp. 1146-1151, 1999.

Dirk Van Eester obtained his Master degree of Mathematics and Mathematical Physics summa cum laude at KULeuven in 1983. He worked under a Marie-Curie Fellowship and was based at the Institut fur Plasmaphyzik of the Forschungszentrum Julich (Germany) until he obtained his PhD summa cum laude in 1989, equally at KULeuven. His main focus is on advancing ion cyclotron resonance heating theory and on crosschecking the validity of theoretical predictions against experimental findings. Up to a few months per year, he takes part in experimental magnetic confinement fusion campaigns but dominantly he is based in the Laboratory for Plasma Physics ERM/KMS, Brussels, Belgium.

Maryna Surkova was born in 1987. She received her Master Degree of Experimental Nuclear and Plasma Physics from the 'V. N. Karazin' National University in 2010. In 2010 she joined the department of Applied Physics at Ghent University as a PhD student. She performed numerical and analytical research into application of finite-difference time-domain (FDTD) method in magnetised cold plasma, with focus on modelling electromagnetic plasma waves in fusion devices. In a meantime from 2014 she works at Federal Agency of Nuclear Control (FANC) as an expert in radioactive waste management.

Guido Van Oost graduated in electrotechnical engineering at Ghent University in 1972, and received his PhD degree in engineering physics in 1978 with research on waves in bounded plasmas at LPP-ERM/KMS Brussels. From 1982 till 1999 he worked on RF heating and plasma confinement on the tokamak TEXTOR of the Forschungszentrum Jlich (Germany). Since 1999 he is full professor at Ghent University and Head of the Research Unit Nuclear Fusion. He is Honorary Professor of St. Petersburg State Polytechnic University. He published more than 500 scientific papers. His present research activities are focused on improved magnetic confinement, plasma edge diagnostics, plasma-wall interaction, and materials for fusion reactors. Since 2006 he is the coordinator of an Erasmus Mundus "European Master in Nuclear Fusion and Engineering Physics".

Wouter Tierens was born in 1986. He received his Master Degree of Applied Physics from the University of Gent in 2009. In 2013 he obtained a Ph.D. degree. The subject of his Ph.D. was using time-domain techniques to model interactions between electromagnetic waves and cold and warm magnetized plasmas. He has authored several papers on this topic and related topics. At present, his research focuses on data analysis techniques for DNA analysis.

Daniël De Zutter was born in 1953. He received his M. Sc. Degree in electrical engineering from the University of Gent in 1976. In 1981 he obtained a Ph. D. degree and in 1984 he completed a thesis leading to a degree equivalent to the French Aggrgation or the German Habilitation (both at the University of Gent). He is now a full professor of electromagnetics. His research focusses on all aspects of circuit and electromagnetic modelling of high-speed and high-frequency interconnections and packaging, on Electromagnetic Compatibility (EMC) and numerical solutions of Maxwell's equations. As author or co-author he has contributed to more than 220 international journal papers (cited in the Web of Science) and 250 papers in conference proceedings. In 2000 he was elected to the grade of Fellow of the IEEE. He was an Associate Editor for the IEEE Microwave Theory and Techniques Transactions. Between 2004 and 2008 he served as the Dean of the Faculty of Engineering of Ghent University and is now the head of the Department of Information Technology.

Ivan Pavlenko was born in Sumska region, Ukraine, in 1971. He received the M.S. degree in experimental nuclear and plasma physics and the Candidate of Science degree in plasma physics from V. N. Karazin Kharkiv National University, Kharkiv,Ukraine, in 1994 and 1998, respectively. He was a Post-Doctoral Researcher with Physique Statistique et Plasmas, Universit Libre de Bruxelles, Brussels, Belgium, from 2000 to 2003. Since 2004, he has been an Assistant Professor with the School of Physics and Technology, V. N. Karazin Kharkiv National University. He is the author of a textbook and more than 40 articles. His current research interests include the properties of the surface waves, the propagation of the electromagnetic waves through the thermonuclear plasmas, and synchrotron radiation of the runaway electrons during the thermonuclear fusion experiments.